

AUTOMATED METHODS FOR NEURON SEGMENTATION AND ANALYSIS OF ELECTRON MICROSCOPE IMAGES

Jingyun Chen¹, Heather L. More², Eli Gibson¹, J. Maxwell Donelan², Mirza Faisal Beg¹
¹*Medical Image Analysis Lab, School of Engineering Science, Simon Fraser University.*
²*Locomotion Laboratory, Department of Biomedical Physiology & Kinesiology, Simon Fraser University.*

INTRODUCTION

Quantifying the size, shape, number, and location distribution of axons in peripheral nerves is an important first step in understanding tradeoffs employed in the animal nervous system^[1]. Scanning electron microscope images of nerve cross-sections from animals spanning a wide range of sizes, from shrew to elephant, can be helpful in elucidating these principles. Current methods of labeling axon and myelin (also called segmentation) from these images commonly involve manually labeling each axon, which is extremely time-consuming as a single nerve can contain thousands of axons. In order to make this process more efficient, we developed a computer-assisted neuron segmentation and analysis method.

METHOD

We acquired sciatic nerves samples from a shrew and an elephant, and fixed the samples in a mixture of 4% paraformaldehyde and 1% glutaraldehyde before staining them with osmium tetroxide and embedding them in plastic resin in preparation for imaging. A Bausch & Lomb 2100 Nanolab scanning electron microscope imaged the nerves at a magnification of approximately 1500x to obtain 512x477 pixel images. The microscope scanned at 10 kV using a spot size of 7, the 'low 6' or 'med 4' resolution setting, and the backscatter detector. Shrew and elephant nerves had total diameters of approximately 0.3 mm and 2 cm respectively, with fascicle diameters of approximately 0.2 mm and 0.5 mm respectively.

Our methods can be divided into four main stages: image acquisition, image smoothing, axon labeling, and myelin labeling. In the first stage, we acquired high-resolution electron microscope images of nerve cross-sections. Due to instrument limitations, we could not acquire a single image of the entire nerve cross-section and therefore scanned through the cross-section to obtain a set of overlapping sub-images with identical size and resolution (Figure 1). In this way we made full use of the electron microscope resolution to capture as much information from the cross-section

slices as possible. We developed an algorithm which stitched the sub-images together using normalized cross-correlation^[2] as shown in Algorithm 1.

In the second stage, our algorithm pre-processed the original image by smoothing it to remove noise. Since common convolution algorithms such as Gaussian smoothing or Laplacian smoothing usually smooth object boundaries as well as noise, potentially reducing segmentation accuracy, we used combined morphological operations^[3] and morphological reconstructions^[4] to smooth the original image. This method preserves boundaries while denoising the nerve cross-section, as shown in Algorithm 2.

In the third stage, our algorithm segmented and individually labeled the axons on the pre-processed image. Most axons in our cross-section images are featured as dark areas, each surrounded by a light annulus of myelin. Early studies have reported successful applications of morphological operations in axon segmentation, making use of the geometric characteristics of axons^[5]. Therefore we developed our algorithm based on morphological operations as shown in Algorithm 3.

With Algorithm 3, the majority of axons can be extracted as connected components in the binary image and labeled individually using classic labeling methods^[6]. However, some background areas (i.e. the dark gaps between axons) can be mislabeled as axons because they are also surrounded by myelin of different axons and form connected components on their own. To reduce the mislabeling of connected components as axons we added the following inclusion/exclusion rules:

- a. *Number of pixels in a connected component.* Axons have a finite range of possible sizes – a connected component with size outside this range is a background area.
- b. *Number of myelin annuluses surrounding a connected component.* Axons are only surrounded by one myelin annulus while background areas are surrounded by myelin

annuluses from different axons. This rule requires an initial labeling of myelin.

- c. *Shape of a connected component.* The shape of normal axons is close to roundness, while background areas can have arbitrary shape. There are different ways to measure the “degree of roundness”. We used the parameter $R = N_B/N$, where N_B is the number of pixels on the boundary of a connected component, and N is the total number of pixels in that component. With size limited by rule a., components with shape close to round have small R , while components with concave-convex shape have large R .

We set the parameters in above rules (such as sizes, numbers) by our prior knowledge to the nerve units’ physical prosperities. Using these rules, our algorithm removed the majority of mislabeled background areas from axon label set.

In the fourth stage, our algorithm labeled the myelin annulus. On the cross-section image, myelin is featured as a higher-intensity annulus surrounding an axon with lower intensity values. We applied a boundary detection method known as the star algorithm^[7] to find the myelin annulus around each axon. This algorithm starts with a seed point at the geometric center of the axon and computes the gradient of image intensity values in a given radial direction. The first gradient change indicates the beginning of the myelin annulus, and the second gradient change indicates the end. The algorithm is repeated in each direction until all 360° are searched and all the pixels in the boundary annulus are labeled. We implemented external constraints such as myelin thickness to prevent the labeled myelin from “leaking” into surrounding areas in cases where the myelin boundary was difficult to identify.

RESULTS

We used our algorithm to analyze nerve units of shrew, rat, and elephant. Depending on the size of each nerve, between 6 and 50 sub-images were scanned to result in a stitched image covering the entire nerve cross-section. We implemented our algorithm in Matlab R2009a (Version 7.8.0.347, The MathWorks, Inc. Natick, MA), and implemented morphological operation and reconstruction using the Matlab Image Processing Toolbox™. The typical processing time for a 4-6 million-pixel image on a PC (1.66GHz Pentium M Processor, 1G RAM) was approximately 5 minutes.

The processing results of a sample image are shown in Figures 2 and 3. Most axons and myelin

areas were successfully labeled individually, with only a few small axons with non-round shapes remaining unlabelled. To further reduce the mislabel rate (percentage of false detections plus failed detections), the residual mislabeled areas were manually corrected with a graphic user interface we developed in Matlab. According to our experience in manual correction, the mislabel rate of our automated method is under 10%.

CONCLUSIONS

In this paper we present an automated method for axon and myelin segmentation in scanning electron microscope images of nerve cross-sections. We have used this method to investigate the effect of animal size on axon size and number, in order to gain a deeper understanding of the physiological mechanisms used by small and large animals to control their movements. The method has reduced a large amount of repetitive manual work and has been proven to be well-suited for identifying axons, myelin, and their size characteristics. Future work includes adding more differential rules to further reduce mislabeling and developing machine learning methods to automatically determine external constraints that are currently manually set.

FIGURE AND TABLES

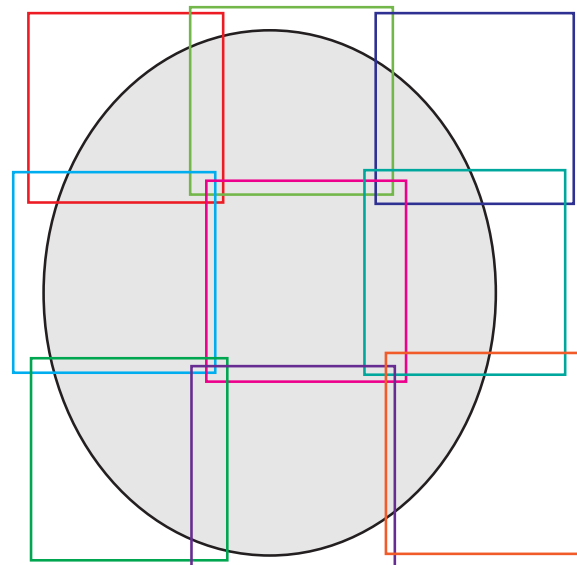


Figure 1: Stitching sub-images (colorful rectangles) to cover a whole nerve cross-section (grey circle).

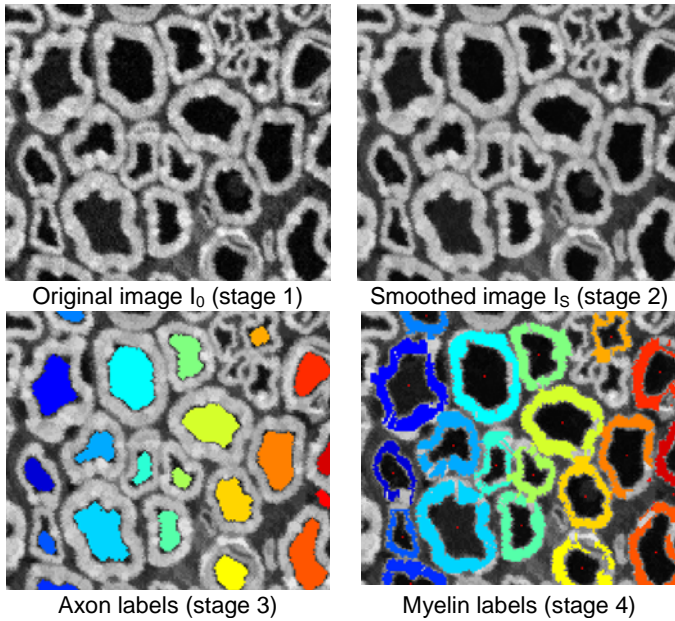


Figure 2: One representative sub-image and processing results of each stage.

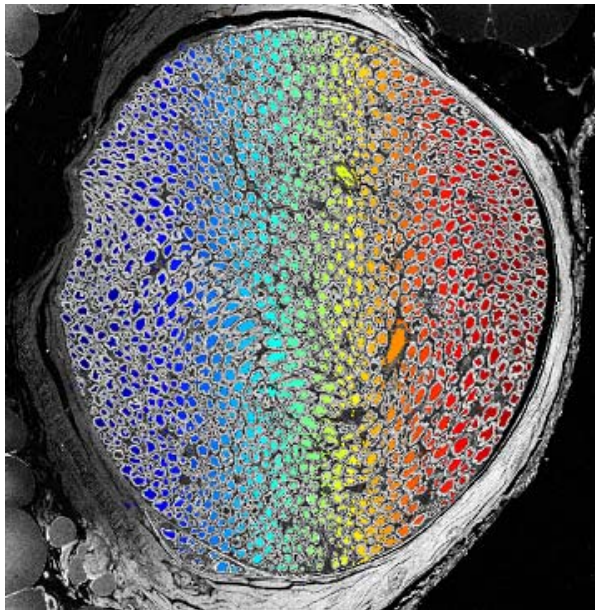


Figure 3: Axon labels (colored areas) for a whole shrew nerve unit.

ALGORITHMS

Algorithm1: Stitching sub-images
 Input: Set of original sub-images I_1, I_2, \dots, I_N .
 Output: Stitched original image I_0

Set iteration number $n = 1$
 While $n < N-1$
 Do
 Let $f = I_n$, i.e. $f(x,y)$ is intensity value location (x,y) in image I_n . Let $t = I_n \cap I_{n+1}$.
 Offset $(u,v) = \underset{u,v}{\text{max}} Y(u,v)$, where

$$\gamma(u,v) = \frac{\sum_{x,y} [f(x,y) - \bar{f}_{u,v}] [t(x-u, y-v) - \bar{t}]}{\left[\sum_{x,y} [f(x,y) - \bar{f}_{u,v}]^2 \sum_{x,y} [t(x-u, y-v) - \bar{t}]^2 \right]^{0.5}}$$

 Set $I_0 = I_n \cup I_{n+1}$ with offset (u,v)
 Set $n = n+1$
 End

Algorithm 2: Pre-processing images

Input: Original image I_0 .

Output: Smoothed image I_S .

$I_E = \text{erode}(I_0)$

$I_{R1} = \text{reconstruct}(I_E \text{ as marker}, I_0 \text{ as mask})$

$I_D = \text{dilate}(I_0)$

$I_{R2} = \text{reconstruct}(I_D^C \text{ as marker}, I_{R1}^C \text{ as mask})$

$I_S = I_{R2}^C$

where $\text{erode}()$, $\text{dilate}()$, and $\text{reconstruct}()$ are morphological erosion, dilation, and reconstruction, respectively, and f^c is the complement image of f .

Algorithm3: Segmenting axons

Input: Pre-processed image I_S

Output: Binary segmentation of axons I_{AXON} .

$I_{SB} = \text{threshold}(I_S)$

$I_{AXON} = \text{open}(I_{SB})$

where $\text{threshold}()$ is the conversion of an intensity image into binary image using a threshold, and $\text{open}()$ is the morphological open operation.

ACKNOWLEDGEMENTS

The authors would like to thank Dr. Parvaneh Saeedi from School of Engineering Science, Simon Fraser University for her constructive advices on the myelin segmentation algorithm.

REFERENCES

- [1] H.L. More, J.R. Hutchinson, D.F. Collins, D.J. Weber, S.K.H. Aung, and J.M. Donelan, "Scaling of sensorimotor control in terrestrial mammals," *Proceedings of the Royal Society B (under review)*
- [2] J. P. Lewis, "Fast Template Matching", *Vision Interface 95, Quebec City, Canada*, pp. 120-123, 1995.
- [3] R. Haralick, and L. Shapiro, "Computer and robot vision", *Addison-Wesley*, vol. 1, pp. 158-205, 1992.
- [4] L. Vincent, "Morphological grayscale reconstruction in Image analysis: applications and efficient algorithms", *IEEE Transactions on Image Processing*, vol. 2, No. 2, pp. 176-201, April, 1993.
- [5] R. C. Vogt, and A.A. Mich, "Method of extracting axon fibers and clusters", *US Patent No. 5850464*, 1998.

- [6] R. Haralick, and L. Shapiro, "Computer and robot vision", *Addison-Wesley*, vol. I, pp. 28-48, 1992.
- [7] W. Yao, J. Tian, B. Zhao, N. Chen and G. Qian, "Star algorithm: Detecting the ultrasonic endocardial boundary automatically" *Ultrasound in Medicine & Biology*, vol 30, Issue 7, pp. 943-951, July 2004.